

## BRAGG DIFFRACTION IMAGING OF MAGNETIC CRYSTALS: NEW RESULTS FROM NOVEL BEAMS

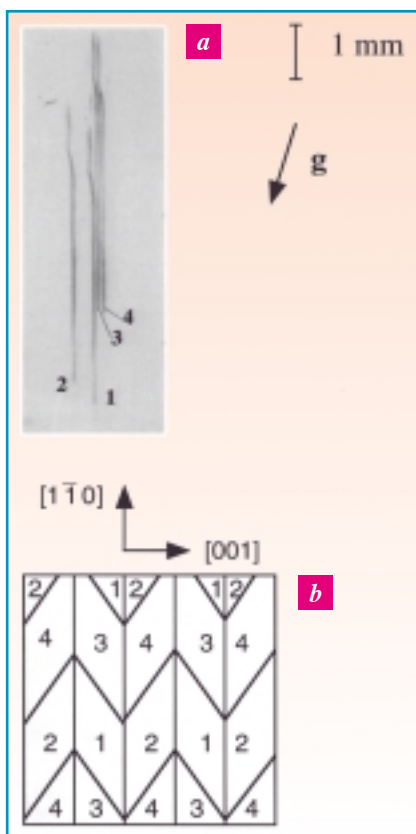
C. MEDRANO <sup>1,2</sup>, I. MATSOULI <sup>1,3</sup>,  
J. I. ESPESO <sup>1,4</sup>, V. V. KVARDAKOV <sup>5</sup>,  
M. SCHLENKER <sup>6</sup>, J. BARUCHEL <sup>1</sup>

- 1 ESRF
- 2 UNIV. ZARAGOZA, SPAIN
- 3 UNIV. WARWICK, UK
- 4 UNIV. CANTABRIA, SANTANDER, SPAIN
- 5 KURCHATOV INSTITUTE, MOSCOW, RUSSIA
- 6 LAB. LOUIS NÉEL, CNRS, GRENOBLE, FRANCE

### INTRODUCTION

Bragg diffraction x-ray imaging (x-ray topography) produces direct-space images of crystal defects, domains, or just thickness variations in single crystals, via the inhomogeneous intensity of the Bragg-diffracted beams.

*Fig. 1: a) Section topograph in white beam. Low temperature phase of magnetite.  $T = 110\text{ K}$ ,  $B = 300\text{ mT}$ ; 593 reflections,  $\lambda = 0.3\text{ \AA}$ ,  $\mu t \approx 1$ . b) Model for the monoclinic twins in the sample.*



The advent of synchrotron radiation brought high intensity making real-time imaging possible and at high energy machines a large flux of high energy photons, allowing the observation of thick samples in transmission geometry. On third-generation machines, the small emittance of the source again provides new possibilities. Because image blurring remains small even when the detector is placed far from the sample, particularly at the long (145 m) beamline of ID19, the specimen-detector distance becomes a new adjustable parameter. It extends the range of options traditionally available: white beam vs monochromatic beam imaging, projection vs section topography, selection of wavelength and choice of the Bragg reflection.

We briefly present results obtained at the ESRF, using beamline ID19, on magnetic materials: the oldest magnetic material known, magnetite  $\text{Fe}_3\text{O}_4$ ; hæmatite  $\alpha\text{-Fe}_2\text{O}_3$ , manganese phosphide  $\text{MnP}$ , with a wealth of magnetic phases; and iron borate  $\text{FeBO}_3$ . Although the scattering process used is Thomson (charge) scattering and provides information on the magnetic moments only via the lattice distortion, quite spectacular results were obtained.

### PROBING SYMMETRY: THE LOW-TEMPERATURE PHASE OF MAGNETITE

Magnetite, cubic above its Curie point and a ferrimagnet at room temperature, exhibits at 120 K a transition affecting its electric and magnetic properties. Below this Verwey transition, the crystal symmetry is either monoclinic or even triclinic, implying that a single crystal splits into many domains or twins. Magnetite is also magnetoelectric at low temperature,

with ferroelectricity coupled with ferrimagnetism.

The domain structure was followed across the transition, using white-beam topography. The least complicated situation prevailed, as expected, when the transition was passed in a magnetic field favouring one of the easy  $\langle 001 \rangle$  magnetization directions, or the nearest easy directions  $[001]$ . Even then, however, so many domains were superimposed on any projection topograph that, contrary to standard usage, this provided no overall view. White beam section topographs, in which the effectively investigated region was a ribbon, some  $20\text{ }\mu\text{m}$  thick across the  $0.8\text{ mm}$  thick sample, provided clues to the coexisting domains, their shape and arrangement.

Figure 1a shows a typical result, corresponding to one Laue spot, to be compared with the single straight line a single domain would yield. Unraveling this data involved first the determination of matching lines, associated with adjacent domains in the specimen; then the measurement of the geometric splitting of the corresponding lines associated with the relative rotation of the lattice planes for a number of Laue spots; and comparison with calculation. The outcome is a plausible model, shown in Figure 1b, of monoclinic domains, with all walls satisfying the conditions of neither magnetic nor electric charge distributions, and no long-range elastic stress. Supplementary contrast is observed, and is the first unambiguous evidence of extra distortions associated with triclinic symmetry.

The ability to vary the sample-to-film distance, to obtain high sensitivity to lattice plane rotation at large (40 cm) distances, and to confirm the assignment of matching elements at smaller distances, proved essential.

*Fig. 2: White beam section topograph on a 1.2 mm thick hematite sample. 21 reflection,  $\lambda = 0.22\text{ \AA}$ ,  $\mu t \approx 0.5$ . Demagnetized state.*

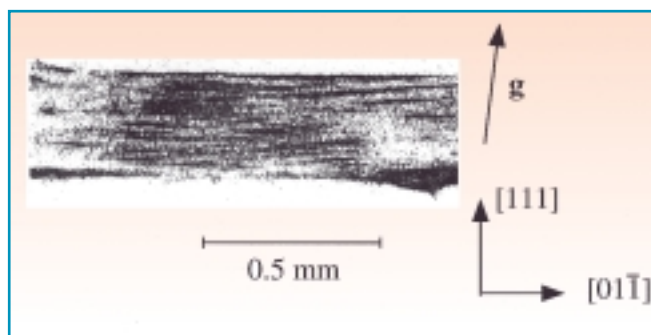
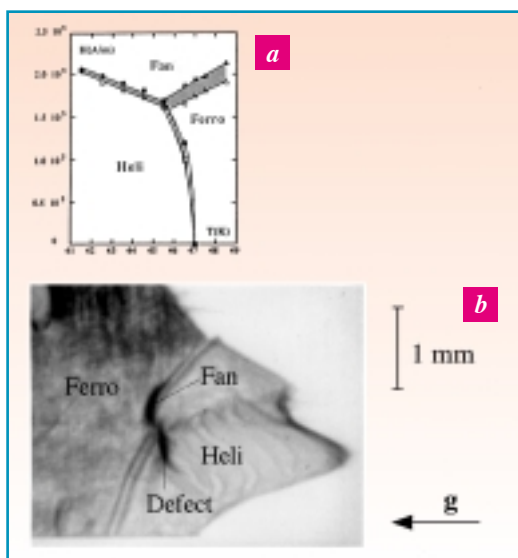




**Fig. 3:** *a) Magnetic phase diagram, indicating the range in applied field of the coexistence on the video monitor. b) White beam topograph at the triple point in MnP. 020 reflection.*



### AN UNUSUAL MAGNETIZATION PROCESS: HÆMATITE

Hæmatite at room temperature is a weak ferromagnet, in which the magnetic moments are almost antiparallel and lie in the low anisotropy basal plane of the trigonal structure. Under an in-plane magnetic field, samples parallel to this (111) plane fail to show domain walls. The white beam section topography investigation of a very good crystal provides the clue to this riddle (Figure 2): the walls are pinned along (111), and magnetization occurs through rotation of the magnetic moments. This is quite different from the standard process prevailing in materials with more sizeable anisotropy, where magnetization would proceed through the displacement of walls, which would furthermore be highly unlikely to take this maximum area orientation.

### MAGNETIC PHASE COEXISTENCE: MANGANESE PHOSPHIDE MNP

Orthorhombic MnP features a magnetic phase diagram with ferromagnetic, helimagnetic, and fan structures all within reach with moderate temperatures and fields. Synchrotron radiation topography can reveal the coexistence of two or three of the magnetic phases because each involves slightly different lattice distortions. In the standard representation, the magnetic phase diagram as an  $H_0, T$  plot shows coexistence lines. The experimental plot in the  $H_0, T$  plane, where  $H_0$  is the applied field, shows bands instead of

lines (Figure 3a). This is related to the different spontaneous magnetization in each phase. A range of values of  $H_0$  corresponds to the same value of  $\mathbf{H} = \mathbf{H}_0 + \mathbf{H}_{\text{dem}}$  because the demagnetizing field  $\mathbf{H}_{\text{dem}}$  changes continuously as one of the coexisting phases grows. In the same way, the triple point is spread into a (small) area in the  $H_0, T$  plane. Figure 3b shows a projection topograph obtained at this triple «point» and a schematic assignment of the various parts of the image to the different phases. One of the noteworthy features is that the fan phase nucleates within the heli-ferromagnetic interface.

### VISUALIZING MAGNETOELASTIC RESONANCES IN THE MHZ RANGE: IRON BORATE

Iron borate is trigonal, isomorphous with hæmatite and features strong magnetoelastic coupling. White beam projection topographs were recorded while a very good quality (111) single crystal plate, 50  $\mu\text{m}$  thick, was excited into an elastic resonance by a 1.3 MHz a.c. magnetic field superimposed on a small perpendicular d.c. field, both in-plane. The vibration of the magnetic moments induces standing acoustic waves. In this imaging mode, the predominant effect is that of lattice plane rotation of maximum amplitude  $\phi_0$ . A membrane type vibration leads to focusing of different components of the beam. Figure 4 shows some of the results obtained from one Laue spot as the excitation amplitude, hence the rotation amplitude  $\phi_0$ , was varied. Very similar pictures (ESRF Highlights 1996-

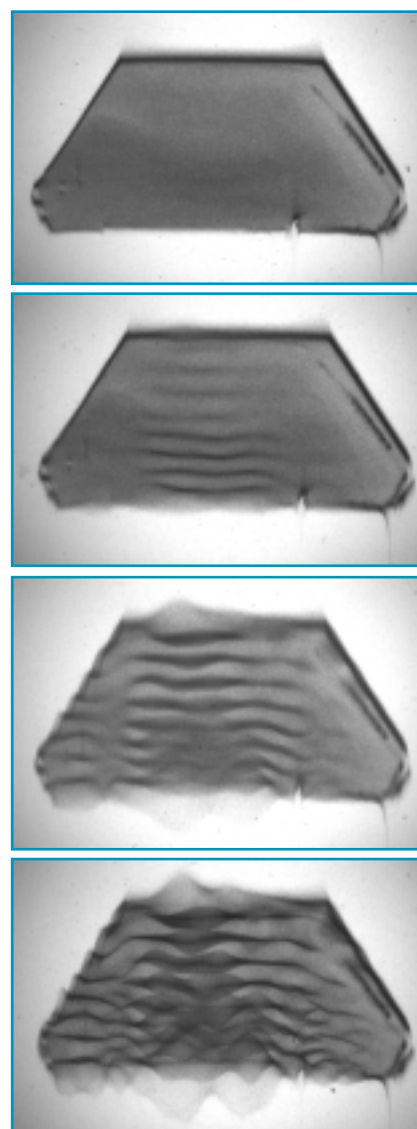


**Fig. 4:** *White beam topographs of the reflection in FeBO<sub>3</sub> 119 cm after the sample as a function of the excitation amplitude; the resonance pattern reveals the time integrated images of the pulsed, focused x-ray beam.*

97) were obtained as a function of the sample-film distance  $L$ . This is in accordance with the formal theoretical description where the relevant parameter is the product  $L\phi_0$ , and again points to the importance of the sample-to-detector distance as a new free parameter provided by the small emittance at the ESRF. Such an experiment gives access to the main characteristics of the vibration: amplitude, shape, polarization, wavelength and sound velocity. In addition this effect could be used to obtain a high frequency pulsed, «monochromatic», and focused x-ray beam. ■